REDVET - Revista electrónica de Veterinaria - ISSN 1695-7504
Vol 25, No. 1 (2024)
http://www.veterinaria.org
Article Received: Revised:Accepted:

Nano-Selenium Enriched Chitosan Particles For Fish Feed: Synthesis And Evaluation

Latha Srinivasan[1], Kumaran Subramanian[1,2]*

[1]Centre for Drug Discovery and Development, Faculty of Bio and Chemical Sciences, Sathyabama Institute of Science and Technology, Chennai, Tamil Nadu, India
[2]Research Department of Microbiology, Sri Sankara Arts and Science College, Kanchipuram, Tamil Nadu, India

***Corresponding Author:** Kumaran Subramanian
Email: kumaransubramanian23@gmail.com

Abstract
Background: Sustainable aquaculture depends on innovative feed strategies that enhance fish growth, health, and environmental safety. Chitosan and selenium nanoparticles have shown promise as bioactive supplements due to their antioxidant, antimicrobial, and immunostimulatory effects. This study aimed to synthesize nano-selenium-enriched chitosan particles (Cs-SeNPs) and evaluate their potential in fish feed formulation for Oreochromis niloticus (Nile tilapia).
Methods: Chitosan-selenite nanoparticles were synthesized using the ionotropic gelation method and characterized by UV–Vis spectroscopy, FTIR, SEM, XRD, and zeta potential analyses. The nanoparticles were incorporated into fish feed at varying concentrations and administered to tilapia over 45 days. Growth parameters, feed conversion ratio (FCR), protein efficiency ratio (PER), and immune responses were measured and statistically analyzed using ANOVA.
Results: The Cs-SeNPs displayed spherical morphology, high colloidal stability (zeta potential −36.4 mV), and distinct selenium incorporation confirmed by EDX. Fish fed Cs-SeNP-supplemented diets exhibited significant improvements in weight gain, specific growth rate, and protein efficiency compared to controls ($p < 0.05$). Enhanced lysozyme activity and phagocytic response indicated immune stimulation. The combined chitosan–selenium formulation also showed antimicrobial effects against common fish pathogens.
Conclusion: Nano-selenium-enriched chitosan particles effectively improve growth performance, feed efficiency, and immune function in Nile tilapia, demonstrating potential as a sustainable feed additive for aquaculture. These findings support further exploration of Cs-SeNPs as functional nanonutrients to enhance fish health and productivity.

Keywords: Chitosan nanoparticles, Selenium nanoparticles, Nile tilapia, Aquaculture feed, Antioxidant activity, Nanonutrition

Introduction

Aquaculture, the farming of aquatic species such as fish, molluscs, crustaceans, and aquatic plants, has become one of the fastest expanding food-producing sectors globally (Anderson et al., 2017; Mustafa et al., 2021). At present, close to half of the seafood consumed worldwide is derived from aquaculture, making the sector vital for food security and nutrition, particularly in areas heavily dependent on fish as a major source of protein (Phan et al., 2009; Bostock et al., 2010; Mair et al., 2023). Nevertheless, intensive practices can lead to ecological problems, including habitat degradation, water contamination, and heavy reliance on wild-caught fish for feed. Since feed accounts for 50–70% of production costs, the development of sustainable, balanced, and cost-efficient alternatives remains one of the major priorities for long-term growth (Hoerterer et al., 2022; Naylor et al., 2009).

Progress in Aquaculture Feed Formulation

Conventional feeds based on fish meal and fish oil are increasingly being substituted with alternatives such as soybean meal, insect protein, algae, and microbial sources. These innovations not only address sustainability concerns but also maintain growth and feed conversion performance (Hasan et al., 2009; Hardy, 1999; Zhou et al., 2018). More recently, integrated approaches such as “nutritious pond feeds” have been introduced to enhance both fish growth and the microbial ecosystem within rearing ponds, thereby improving fish health and water quality (Olsen, 2011; Fiorella et al., 2021).

Role of Nanotechnology in Aquaculture

Nanotechnology has emerged as a novel tool to enhance feed utilization, growth, and disease resistance in fish while reducing environmental impacts (Peters et al., 2016; Sharjeel et al., 2024). Metal-based nanoparticles, including zinc, silver, and copper, have demonstrated improved nutrient uptake, antimicrobial activity, and growth responses (Kumar et al., 2023; Thangapandiyan& Monika, 2020; De Silva et al., 2021; Dawood et al., 2020). Lipid-based carriers such as nano-emulsions, solid lipid nanoparticles (SLNs), and nanostructured lipid carriers (NLCs) provide effective delivery of sensitive compounds like fatty acids and vitamins (Abd El-Hamid et al., 2021; Korni et al., 2023; Patridge et al., 2019).

Likewise, polymeric nanoparticles—especially chitosan and PLGA—are increasingly employed for nutrient encapsulation, vaccine delivery, and controlled drug release (Ghanbary et al., 2022; Joshi et al., 2022). Other nanoparticle systems, including silica and calcium phosphate, are being evaluated for their roles in antioxidant defense and skeletal development (Bashar et al., 2021; Terzioglu et al., 2018).

Chitosan Nanoparticles (CNPs)
Chitosan, derived from crustacean shells, is biodegradable, biocompatible, and known for its antimicrobial properties. When converted into nanoparticles, it gains added advantages such as muco-adhesion and efficient nutrient encapsulation, making it a highly versatile material (Divya & Jisha, 2018; Bashir et al., 2022). Beyond aquaculture, CNPs are widely studied for applications in drug delivery, agriculture, food preservation, and water treatment (Garg et al., 2019; Chouhan & Mandal, 2021; Wang et al., 2023; Olivera et al., 2016). In fish feed, they have been shown to improve growth performance, immune activity, and feed utilization while reducing antibiotic dependence (Kumaran et al., 2020; Akter et al., 2023).

Selenium Nanoparticles (SeNPs)
Selenium is a trace mineral with essential roles in antioxidant defense and immune regulation. In nanoparticle form, selenium becomes more bioavailable and effective, while lowering toxicity risks associated with conventional supplementation (Xiao et al., 2023). In aquaculture, SeNPs have improved growth, feed conversion, and disease resistance in species such as tilapia and carp (Sarkar et al., 2015; Dawood et al., 2021). They also have wider applications in medicine, agriculture, and food preservation due to their antioxidant and antimicrobial properties (Bisht et al., 2022; Vijayakumar et al., 2022; Bano et al., 2021; Holmes & Gu, 2016).

Chitosan–Selenium Nanoparticle Combinations
The combination of CNPs with SeNPs has gained attention for use in Nile tilapia diets. Together, they enhance selenium stability, improve absorption, and provide controlled release, which results in better antioxidant activity, immune responses, and overall survival rates (Yazhiniprabha et al., 2022; Abd El-Naby et al., 2020; Abd-Elraoof et al., 2013; Chen et al., 2022). This dual supplementation has also been linked to improved muscle quality and resistance to stress and pathogens (Abdel-Ghany & Salem, 2020; Krishnaraj et al., 2022).

Nile Tilapia (Oreochromis niloticus)
Nile tilapia remains one of the most commercially important species in global aquaculture due to its adaptability, fast growth, and nutritional value (Gonzales & Brown, 2006; Adel et al., 2015). It is extensively used as a research model in aquaculture nutrition, toxicology, and genetics (Munguti et al., 2022; Leonard & Skov, 2022; Tesfahun& Temesgen, 2018). Efforts such as the GIFT breeding program have produced strains with significantly higher growth rates (El-Sayed & Fitzsimmons, 2023), while advances in feed formulations—ranging from plant-based diets to nanoparticle-based additives—have improved feed efficiency, sustainability, and health outcomes (El-Sayed, 2002; Nyakeya et al., 2020; Samrongpan et al., 2019).

MATERIALS AND METHODS

Synthesis and Characterization of Chitosan-Selenite Nanoparticles

Materials and reagents
Chitosan (85% deacetylation, Mw 50–190 kDa), Sodium selenite (Na_2SeO_3) Sodium triphosphate (TPP) and Acetic acid were procured from Sigma Aldrich India. All the chemicals and reagents used in the present study are of analytical grade with 99.9% purity standard.

Preparation of Chitosan-selenite nanoparticles
Chitosan-selenite nanoparticles were synthesized using the ionotropic gelation technique. To begin, a chitosan solution (2.5 mg/mL, pH 4.6) was prepared by dissolving chitosan in a 1% (w/v) acetic acid solution, followed by continuous stirring at room temperature for 6 hours. Subsequently, a sodium selenite aqueous solution (0.6 mg/mL) was introduced dropwise into the chitosan solution under stirring conditions at 500 rpm for 2 hours.
Next, a tripolyphosphate (TPP) aqueous solution (0.25 mg/mL) was added dropwise to the chitosan-sodium selenite mixture, and the suspension was stirred for another 2 hours to form nanoparticles. The resulting suspension was then subjected to sonication using a Sonic Wave CD-2800 ultrasonic cleaner (60 W, Newtown, CT, USA) for 15 minutes. Following sonication, the nanoparticle suspension was centrifuged at 13,000 rpm for 30 minutes. Finally, the collected pellet was lyophilized to obtain chitosan-selenite nanoparticle (Cs-Se NPs) powder.

Characterization of Chitosan-selenium nanoparticles

UV-Vis Spectroscopy Analysis

The optical properties of the synthesized chitosan-selenium nanoparticles (Ch-SeNPs) were evaluated using UV-visible (UV-Vis) spectroscopy to confirm their formation and stability. UV-Vis analysis was performed with a spectrophotometer (Thermofisher, USA), scanning the absorption spectra over a wavelength range of 200–700 nm.

To prepare the sample for analysis, a stable suspension of Ch-SeNPs was obtained by dispersing the nanoparticles in distilled water through sonication for 10 minutes to ensure uniform dispersion. The sample was transferred to a clean quartz cuvette with a 1 cm path length. Distilled water was used as the blank for baseline correction during the measurements. The UV-Vis spectrum of the Ch-SeNPs was carefully analyzed to identify characteristic absorption peaks. Depending on particle size, shape, and capping agents synthesized nanoparticles exhibit a surface plasmon resonance (SPR) peak. The presence of the peak confirmed the successful synthesis of selenium nanoparticles stabilized by chitosan.

In addition to the confirmation of nanoparticle synthesis, the spectrum was monitored for any shifts or changes in the absorbance peak over time to evaluate the stability of the Ch-SeNPs. A consistent absorption profile without significant shifts or decreases in intensity indicated good colloidal stability and minimal aggregation of the nanoparticles. This technique provided a rapid and reliable means of characterizing the optical properties of the Ch-SeNPs, supporting their potential application in the desired fields.

Fourier-transform infrared spectroscopy (FTIR)

FT-IR spectroscopy (Bruker-2000 USA) was used to analyze the Cs-SeNPs, covering a frequency range from 4000 to 500 cm^{-1}. The atomic intuition of all the tests, counting manufactured polymer powdered and hydrogel movies arranged employing an arrangement casting strategy, was measured utilizing Fourier change infrared (FTIR) spectroscopy. For the analysis, a small amount of freeze-dried Ch-SeNPswas finely ground and mixed with potassium bromide (KBr) in a 1:100 ratio to form a uniform pellet. The KBr pellet was prepared using a hydraulic press under high pressure. The prepared pellet was then placed in the sample holder of the spectrometer for scanning.

The resulting FT-IR spectra were analyzed to identify characteristic absorption bands corresponding to various functional groups. Peaks in the 3200–3500 cm^{-1} range were attributed to the O-H and N-H stretching vibrations, indicative of hydroxyl and amine groups present in chitosan. The absorption band near 2900 cm^{-1} was assigned to C-H stretching vibrations. Changes in the fingerprint region (600–900 cm^{-1}) confirmed the presence of selenium, suggesting interactions between chitosan and selenium nanoparticles. Additional shifts or changes in the intensity of peaks, particularly in the region around 1000–1600 cm^{-1}, indicated the binding of selenium to chitosan through functional groups such as amino ($-NH_2$) or hydroxyl (-OH) groups. This analysis validated the successful stabilization of selenium nanoparticles by chitosan, highlighting the role of chitosan as a capping agent and its potential functionalization for various applications.

Scanning electron microscopy (SEM)

The surface morphology and structural details of the synthesized chitosan-selenium nanoparticles (Ch-SeNPs) were analyzed using a Scanning Electron Microscope (SU8010, Hitachi, Tokyo, Japan) operated at an accelerating voltage of 3.0 kV.

To prepare the sample for SEM imaging, a drop of the Ch-SeNP suspension was placed onto a clean aluminum stub and air-dried at room temperature. The dried sample was then coated with a thin layer of gold using a sputter coater to enhance electrical conductivity and reduce charging effects during imaging. The SEM micrographs provided detailed information on the size, shape, and surface morphology of the nanoparticles. The Ch-SeNPs were expected to exhibit a spherical or nearly spherical shape, with uniform dispersion across the field of view. Any instances of aggregation or clustering were also noted, offering insights into the stability and dispersity of the nanoparticles.

The high-resolution images obtained at 3.0 kV allowed for precise visualization of the nanoparticle surface, confirming the successful synthesis and stabilization of selenium nanoparticles by chitosan. These observations were used to complement data from other characterization techniques and to validate the structural properties of the Ch-SeNPs.

X-Ray Diffraction (XRD) Analysis

The crystalline structure and phase composition of the synthesized chitosan-selenium nanoparticles (Ch-SeNPs) were analyzed using X-ray Diffraction (XRD). The analysis was conducted using an X-ray diffractometer (Bruker D8 Advance,USA) equipped with Cu-Kα radiation (λ = 1.5406 Å), operating at a voltage of 40 kV and a current of 30 mA.

The freeze-dried Ch-SeNP powder was spread uniformly onto a sample holder, ensuring a smooth and even surface. XRD patterns were recorded in the 2θ range of 10°–80° at a scanning speed of 2° per minute and a step size of 0.02°.

The obtained diffraction patterns were analyzed to identify characteristic peaks corresponding to selenium nanoparticles and to evaluate their crystalline nature. Peaks in the XRD spectrum were compared with standard reference data from the Joint Committee on Powder Diffraction Standards (JCPDS) database to confirm the crystalline phases of selenium.

The broadening of diffraction peaks was used to estimate the crystallite size of the nanoparticles using the Debye-Scherrer equation:

$D=k\lambda/\beta\cos\theta$
Where:

- D is the crystallite size (nm),
- k is the shape factor (typically 0.9),
- λ is the X-ray wavelength (1.5406 Å for Cu-Kα),
- β is the full-width at half maximum (FWHM) of the diffraction peak (in radians),
- θ is the Bragg angle (in degrees).

This analysis confirmed the crystalline nature and size of the selenium nanoparticles, providing essential structural information for further validation of the synthesis process.

Dynamic Light Scattering (DLS) and Zeta Potential Analysis

The mean diameter and zeta potential (ZP) of the synthesized chitosan-selenium nanoparticles (Ch-SeNPs) were measured using a dynamic light scattering (DLS) particle size analyzer (ZetaSizer Nano ZS ZEN3600, Malvern Instrument; Particle Sizing Systems, Inc., Santa Barbara, CA).

To prepare the samples for DLS analysis, a 100-fold serial dilution of the Ch-SeNP suspension was performed using deionized water to achieve a suitable concentration for measurement. The diluted sample was then transferred to a disposable polystyrene cuvette for particle size measurement, while the zeta potential was analyzed using a folded capillary cell. The DLS measurements provided the hydrodynamic diameter (mean particle size) and the polydispersity index (PDI), which indicated the uniformity of the nanoparticle size distribution. The zeta potential values were used to assess the surface charge of the nanoparticles, which reflects their colloidal stability. A higher absolute zeta potential value indicated greater electrostatic stabilization, reducing the likelihood of aggregation in suspension. This analysis confirmed the size distribution and stability of the Ch-SeNPs, offering critical insights into their suitability for subsequent applications.

EDX Analysis

The Energy Dispersive X-ray (EDX) analysis was performed to determine the elemental composition of the synthesized selenium nanoparticles (SeNPs) and the chitosan-based nanocomposites. The analysis was conducted using a scanning electron microscope (SEM) equipped with an EDX detector, which allowed for the identification and quantification of the elements present in the nanoparticles.

The EDX spectrum of SeNPs revealed a prominent peak corresponding to selenium, confirming the successful synthesis of SeNPs. Additional peaks corresponding to oxygen (O) and carbon (C) were also observed, which are indicative of the presence of the capping agent, likely derived from the polysaccharide-protein complex (PSP) used during the synthesis. These results support the formation of stable SeNPs with a characteristic elemental profile.

For the Ch-SeNP nanocomposite, the EDX spectrum showed peaks for selenium, carbon, nitrogen (N), and oxygen, further confirming the successful incorporation of SeNPs into the chitosan matrix. The presence of nitrogen, a key element in the chitosan structure, was notably evident, demonstrating the integration of chitosan with the nanoparticles.

Growth performance of *Oreochromis niloticus* using prepared nanoparticle feeds

Feed Preparation and Supplementation

For each experimental treatment, the fish feed was carefully prepared using specific formulations tailored to meet the nutritional requirements of *Oreochromis niloticus*. The base feed ingredients consisted of soybean meal, fish meal, groundnut cake, wheat flour, rice bran, and starch, which were selected to provide essential nutrients for optimal fish growth and health. These ingredients were thoroughly mixed with lukewarm water to form a consistent mixture. To enhance the feed's nutritional profile, corn oil, vitamins, and essential minerals were added. For the experimental groups, nanoparticles such as chitosan or selenium nanoparticles were incorporated into the feed by replacing a portion of the base feed components at a specific ratio (1:1 w/v). The mixture was thoroughly blended to ensure uniform distribution of the nanoparticles throughout the feed. The final mixture was shaped into pellets using a pelletizer, dried at 40°C to remove excess moisture, and stored in airtight containers to prevent degradation, nutrient loss, or moisture absorption. This preparation method ensured the feed was nutritionally balanced, stable, and suitable for experimental use.

REDVET - Revista electrónica de Veterinaria - ISSN 1695-7504
Vol 25, No. 1 (2024)
http://www.veterinaria.org
Article Received: Revised:Accepted:


Fig 1a: Materials for fish diet preparation

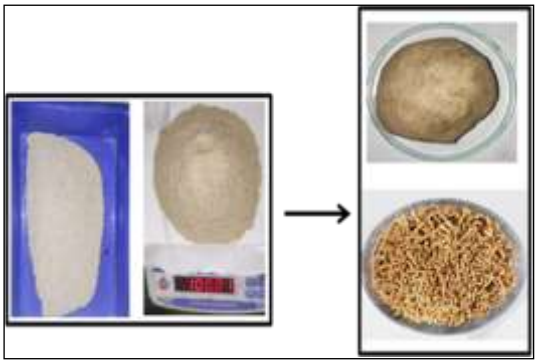
Fig 1b: Paste formation and pellet making

Initial Parameters

Before the commencement of the experiment, the initial weight and length of all fish were recorded. The fish were measured using a digital scale for weight determination (accurate to the nearest 0.01 g) and a measuring board for length (measured from the tip of the snout to the end of the caudal fin). These initial measurements were used to calculate the weight gain and length gain at the end of the study.

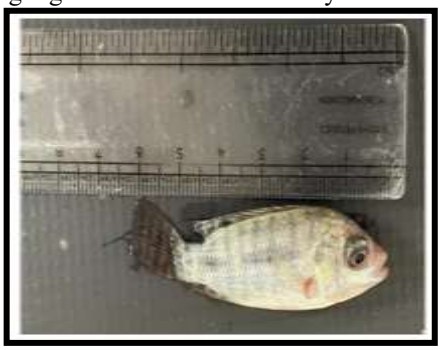

Fig 3A: Initial length of Fish Tank 2Fig 3B: Initial length of Fish Tank 3

Feeding and Tank Maintenance

The fish were fed twice daily, once in the morning and once in the afternoon, at a rate of 3% of their body weight. The feeding rate was adjusted daily based on the observed growth, ensuring that fish received adequate nutrition throughout the study. The fish were maintained under controlled conditions with the following water quality parameters: water temperature was kept at 28°C, pH was maintained at 7.5, and dissolved oxygen levels were kept between 6 and 8 mg/L. These conditions were regularly monitored to ensure the health and well-being of the fish.

Each tank was equipped with a filtration system to maintain optimal water quality, and 20% of the water was changed every two days to prevent the buildup of waste products. The water quality parameters were measured at regular intervals, and any necessary adjustments were made to maintain the ideal conditions for fish growth.

Experiment of treatment groups

The experiment was designed with three treatment groups, each consisting of six different feed formulations, which were as follows:

1.Experiment 1: *Oreochromis niloticus* fed with feed containing chitosan nanoparticles (ChNPs).
2.Experiment 2: *Oreochromis niloticus* fed with feed containing selenium nanoparticles (SeNPs).
3.Experiment 3: *Oreochromis niloticus* fed with feed containing chitosan-selenium nanoparticles (Ch-SeNPs).

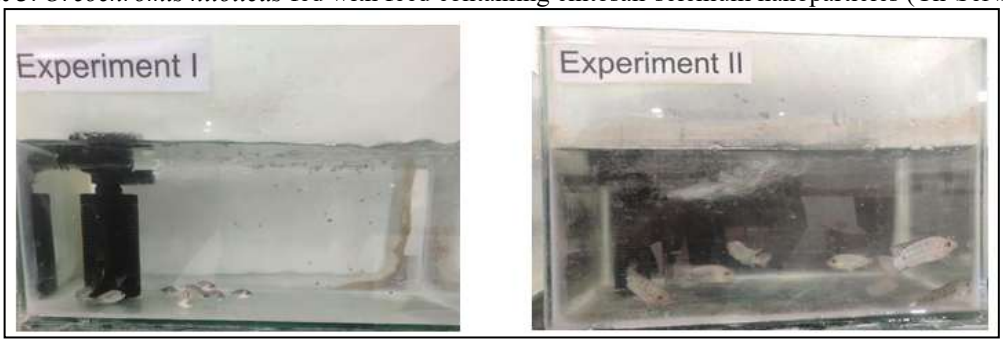

Fig 2A: Experiment 1 **Fig 2B:** Experiment 2

REDVET - Revista electrónica de Veterinaria - ISSN 1695-7504
Vol 25, No. 1 (2024)
http://www.veterinaria.org
Article Received: Revised:Accepted:

Fig 2C: Experiment 3

(Experiment 1: Feed containing chitosan nanoparticles (ChNPs). Experiment 2: Feed containing selenium nanoparticles (SeNPs**),** Experiment 3**:** Feed containing chitosan-selenium nanoparticles (Ch-SeNPs)).
The experimental setup was designed with a total of 18 tanks, where each treatment group was allocated to six tanks, with each tank serving as one replicate. Each tank contained 15 fish, and the total number of fish per treatment group was 90. All fish were selected to be of similar initial size and age to minimize variability in growth performance. The fish were acclimatized to the laboratory conditions for one week before the start of the experiment.

Growth Performance Measurements
At the end of the 45-day experimental period, all fish were harvested and weighed individually using a digital weighing scale. The final body weight of each fish was recorded, and weight gain was calculated by subtracting the initial weight from the final weight. Length measurements were also recorded, using a measuring board, to calculate the length gain by subtracting the initial length from the final length.
In addition to these basic growth parameters, other performance indices, such as specific growth rate (SGR), feed conversion ratio (FCR), and survival rate, were also calculated. The SGR was calculated using the formula:

$$SGR = \left\{ \frac{\ln(W_f) - \ln(W_i)}{T} \right\} \times 100$$

Where Wf is the final weight, Wi is the initial weight, and T is the duration of the experiment in days.
The feed conversion ratio (FCR) was calculated as:

FCR = Total feed consumed / Total weight Gain

Finally, the survival rate of the fish was calculated by dividing the number of surviving fish by the initial number of fish in each tank and multiplying by 100.

Data Analysis
The growth performance data, including final weight, weight gain, length gain, SGR, FCR, and survival rate, were tabulated and subjected to statistical analysis. The data were analyzed using one-way analysis of variance (ANOVA) to compare the differences between the experimental groups. A significance level of $p < 0.05$ was used to determine the statistical significance of the results.
The non-specific immune response, which includes key immune parameters such as total serum protein, lysozyme activity, respiratory burst activity, and phagocytic activity, was measured to assess the effects of the nanoparticle-enriched feeds on the immune function of the fish.

Evaluation of Nonspecific immune response in *Oreochromis niloticus*
The non-specific immune response, which includes key immune parameters such as total serum protein, lysozyme activity, respiratory burst activity, and phagocytic activity, was measured to assess the effects of the nanoparticle-enriched feeds on the immune function of the fish.

1. Total Serum Protein
Blood samples were collected from the caudal vein of the fish using sterilized syringes. The blood was allowed to clot, and the serum was separated by centrifugation at 4°C. Total serum protein concentrations were determined using the biuret method, where the serum was reacted with a biuret reagent, and the absorbance was measured spectrophotometrically at 540 nm.

Blood samples were collected from the caudal vein of *Oreochromis niloticus* using sterilized syringes. Fish were anesthetized with tricaine methanesulfonate (MS-222) before sampling to minimize stress. The collected blood was transferred into anticoagulant-treated tubes (EDTA tubes) to prevent clotting.
For RBC counts, 10 µL of blood was diluted in a 1:200 ratio using Hayem's solution, and the mixture was loaded into a Neubauer hemocytometer. RBCs were counted under a microscope, and the total RBC count was calculated using a standard formula incorporating the dilution factor and hemocytometer grid correction.
For WBC counts, 10 µL of blood was diluted in a 1:20 ratio with Turk's solution, which stains WBC nuclei. The diluted sample was loaded into a Neubauer hemocytometer, and WBCs were counted in the large corner squares. The WBC count was similarly calculated using the dilution factor and grid correction.
The RBC and WBC counts were recorded for each fish and expressed as cells per microliter of blood. The mean and standard deviation of the counts for each treatment group were calculated. Data were statistically analyzed using one-way analysis of variance (ANOVA) to determine differences between the experimental groups. A significance level of $p < 0.05$ was considered statistically significant, and post hoc tests were conducted when necessary.

2. Lysozyme Activity
Lysozyme activity, which is an important component of the innate immune response, was measured using the turbidimetric assay. The serum was incubated with a suspension of *Micrococcus luteus* (a bacterial strain), and the decrease in turbidity, indicative of bacterial lysis, was monitored spectrophotometrically at 450 nm. Lysozyme activity was calculated based on the rate of change in absorbance.

3. Respiratory Burst Activity
The respiratory burst activity of phagocytes was measured using the reduction of nitroblue tetrazolium (NBT) dye. Blood samples were collected, and the white blood cells (WBCs) were isolated and incubated with NBT. The respiratory burst activity was assessed by measuring the reduction of NBT to formazan, which was quantified spectrophotometrically at 540 nm. A higher reduction of NBT reflects increased respiratory burst activity.

4. Phagocytic Activity
The phagocytic activity was assessed by incubating fish blood cells with fluorescently labeled bacteria (*E. coli* or *S. aureus*). After incubation, the percentage of phagocytic cells was determined using flow cytometry or fluorescence microscopy. The number of phagocytic cells was expressed as a percentage of the total leukocyte population. The phagocytic index, representing the number of bacteria engulfed per cell, was also calculated.

5. Sampling and Analysis
Blood samples were collected from a subset of fish (5 per tank) at the end of the 45 days to assess the immune parameters. Sampling was performed under anesthesia using tricaine methanesulfonate (MS-222) to minimize stress on the fish. All immune assays were performed in triplicate, and the results were averaged for analysis.

6. Statistical Analysis
The immune response data, including total serum protein, lysozyme activity, respiratory burst activity, and phagocytic activity, were recorded and analyzed statistically. The data were subjected to one-way analysis of variance (ANOVA) to determine if there were significant differences between the experimental groups. A significance level of $p < 0.05$ was considered statistically significant. If significant differences were observed, Tukey's post hoc test was performed to compare the means between groups.

RESULTS AND DISCUSSION
Characterization of synthesized CsSeNPs using various spectroscopic techniques
UV spectroscopy Analysis

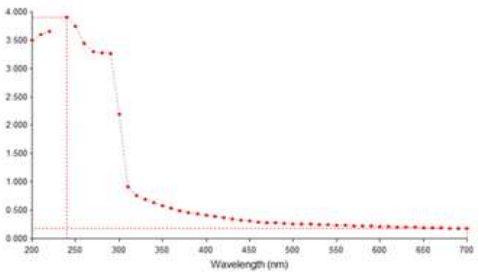

Fig 1A Control

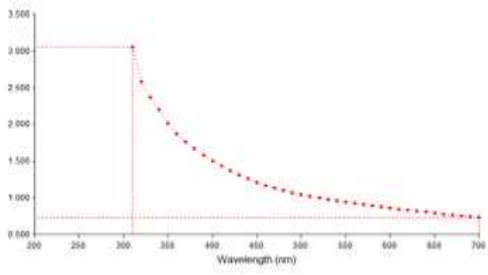

Fig 1B CsSeNPs

REDVET - Revista electrónica de Veterinaria - ISSN 1695-7504
Vol 25, No. 1 (2024)
http://www.veterinaria.org
Article Received: Revised:Accepted:

UV-Vis spectroscopy was performed to characterize the optical properties of the synthesized selenium nanoparticles capped with chitosan (CsSeNPs). The UV-vis analysis was taken from 200-700 nm. The UV-Vis absorption spectrum shows distinct peaks at 375 nm and 549 nm. The peak at 375 nm indicates the excitation of electrons within the chitosan-stabilized selenium nanoparticles, potentially corresponding to the characteristic absorption of selenium nanostructures. The absorption at 549 nm suggests possible aggregation or interactions within the nanoparticle matrix, which may enhance stability and specific optical properties.
These absorption peaks confirm the successful synthesis of selenium nanoparticles within the chitosan matrix, consistent with previous findings on similar nanocomposites. This characteristic UV-Vis profile supports the potential of CsSeNPs for biomedical and antioxidant research applications.

Fourier-transform infrared spectroscopy (FTIR)

FTIR spectroscopy was conducted to identify the functional groups present in the synthesized selenium nanoparticles capped with chitosan (CsSeNPs). The FTIR spectrum exhibits a prominent peak at 3435.56 cm^{-1}, which corresponds to the O-H stretching vibration, indicative of the alcohol group. A peak at 2921.63 cm^{-1} is observed, attributed to the C-H stretching, suggesting the presence of an alkane group within the nanoparticle structure.

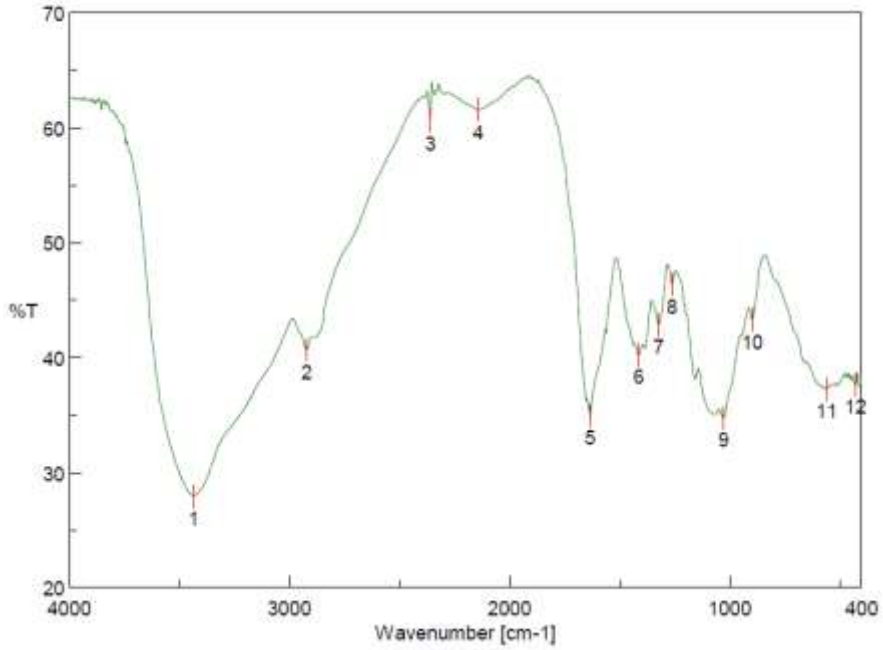

Fig 2: FTIR Spectrum analysis of synthesized nanoparticles

The peak at 2360.44 cm^{-1} likely represents the C≡N stretching vibration, while a signal at 2142.53 cm^{-1} could be indicative of S-C≡N stretching, hinting at an unsaturated functional group as well as a thiocyanate group. A significant absorption band at 1633.41 cm^{-1} is attributed to the C=O stretching vibration, which is characteristic of amide groups in chitosan. Meanwhile, the peaks at 1413.57 cm^{-1} and 1322.93 cm^{-1} are associated with O-H bending and C-F stretching, respectively, further confirming the presence of functional groups from the chitosan and selenium components.
Additional peaks at 1262.18 cm^{-1} and 1027.87 cm^{-1} correspond to C-O and C-N stretching vibrations, characteristic of polysaccharide and amine functionalities, while the peak at 897.70 cm^{-1} suggests the presence of aromatic C-H binding. The peaks at 560.22 cm^{-1} and 428.12 cm^{-1} represent metal-oxygen bonds, supporting the integration of selenium within the nanoparticle matrix.
Overall, the FTIR spectrum confirms the successful incorporation of both chitosan and selenium within the nanoparticle, aligning with the target composition (Figure 3). These findings are consistent with previous studies on selenium-chitosan nanoparticles, which reported similar characteristic peaks, particularly about C=O, C-N, and O-H groups, supporting their potential use as fish feed.

REDVET - Revista electrónica de Veterinaria - ISSN 1695-7504
Vol 25, No. 1 (2024)
http://www.veterinaria.org
Article Received: Revised:Accepted:

Scanning electron microscopy (SEM)

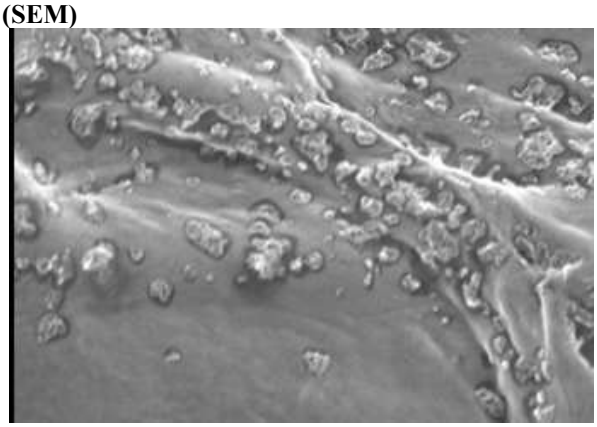

Fig 3A: SEM Analysis of CsSeNPs

Scanning Electron Microscopy (SEM) was conducted to examine the microstructure, size, shape, and dispersion patterns of the synthesized chitosan-selenium nanoparticles (CsSeNPs). Micrographs were acquired at room temperature using an SU8010 model (Hitachi, Tokyo, Japan) with an accelerating voltage of 3.0 kV.
The SEM images revealed that the CsSeNPs exhibit a dense and highly uniform spherical morphology. The nanoparticles were well-dispersed across the field, demonstrating minimal aggregation and uniform nanostructure. This consistent dispersion and morphology indicate successful synthesis, with chitosan effectively stabilizing the selenium nanoparticles. The spherical shape and uniform distribution of the particles suggest that CsSeNPs could offer enhanced surface area and stability, making them suitable for various biomedical and antioxidant applications. These SEM observations provide critical insights into the structural integrity and quality of the synthesized nanoparticles, confirming their potential for applications where nanoscale uniformity is essential.

XRD Analysis

X-ray Diffraction (XRD) analysis was conducted to investigate the crystalline structure and phase composition of the synthesized chitosan-selenium nanoparticles (CsSeNPs). The XRD pattern shows prominent diffraction peaks at 2θ values of 19.70°, 29.68°, and 38.42°, with corresponding d-spacing values of 4.5022 Å, 3.0071 Å, and 2.3408 Å, respectively.

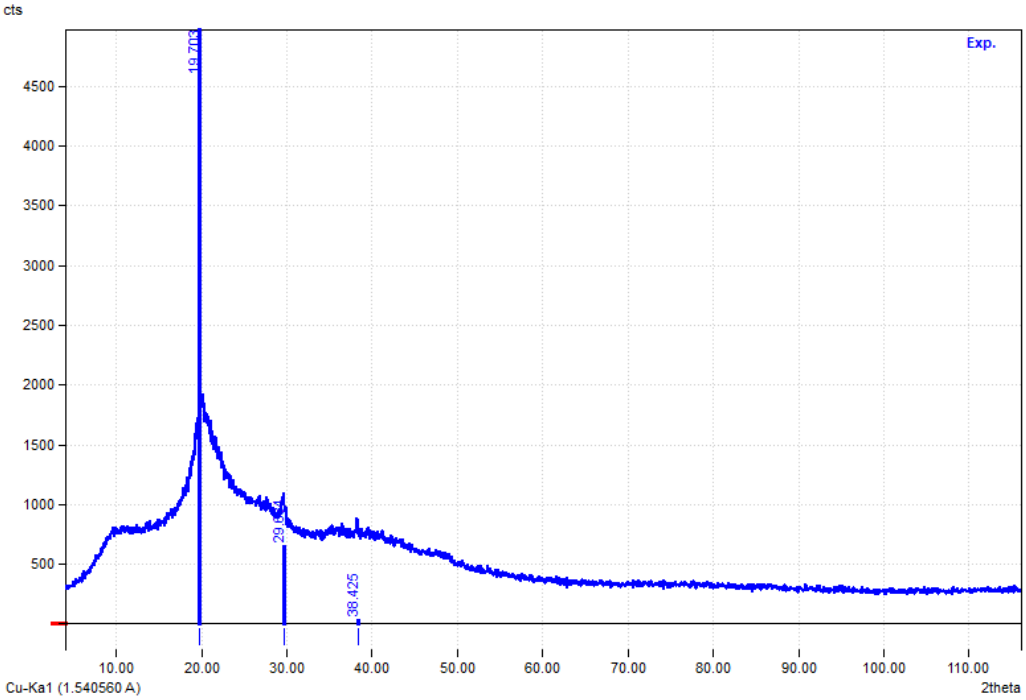

Fig 4: XRD Analysis

The primary peak at 19.70° exhibits the highest intensity (I/I_0 = 1000.00), with a peak area of 4964.81 and a full width at half maximum (FWHM) of 3.9527, indicating a well-defined crystalline phase attributed to the chitosan matrix. The

peak at 29.68° has a relative intensity of 226.32 with an FWHM of 2.2887, suggesting the presence of selenium-based nanostructures. The third peak at 38.42°, with an intensity of 119.17 and a very narrow FWHM of 0.1772, may correspond to minor crystalline domains within the nanoparticle structure.

These XRD results confirm the presence of both chitosan and selenium in the nanocomposite, with a degree of crystallinity that supports the stability and uniformity of the CsSeNPs. The identified crystalline peaks align with the expected diffraction patterns of chitosan-selenium nanocomposites, verifying the successful synthesis and potential for applications requiring well-structured nanoscale materials.

Zeta Potential Analysis

The stability and surface charge of the chitosan-selenium nanoparticles (CsSeNPs) were assessed through zeta potential measurements. The mean zeta potential of the nanoparticles was found to be -36.4 mV, indicating a highly stable colloidal dispersion.

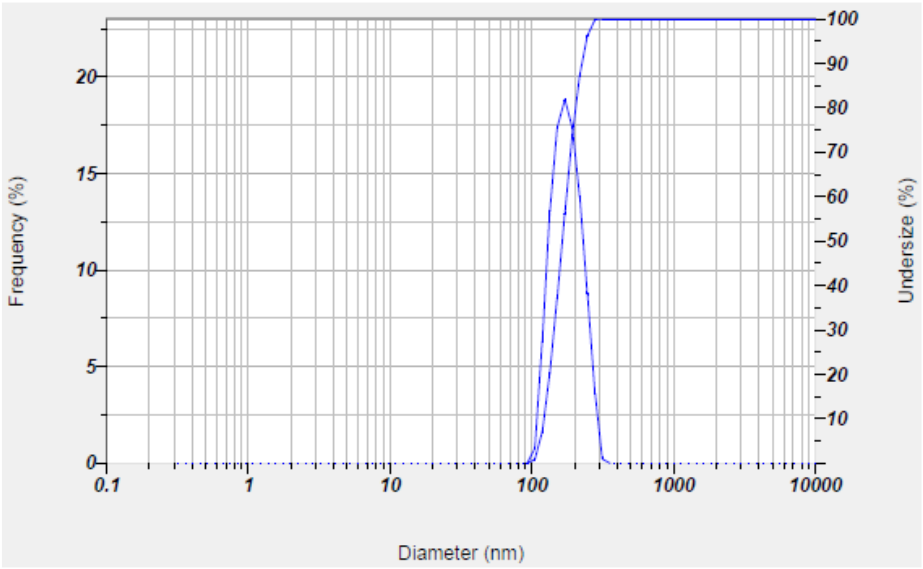

Fig 5 A: Zeta Potential Analysis

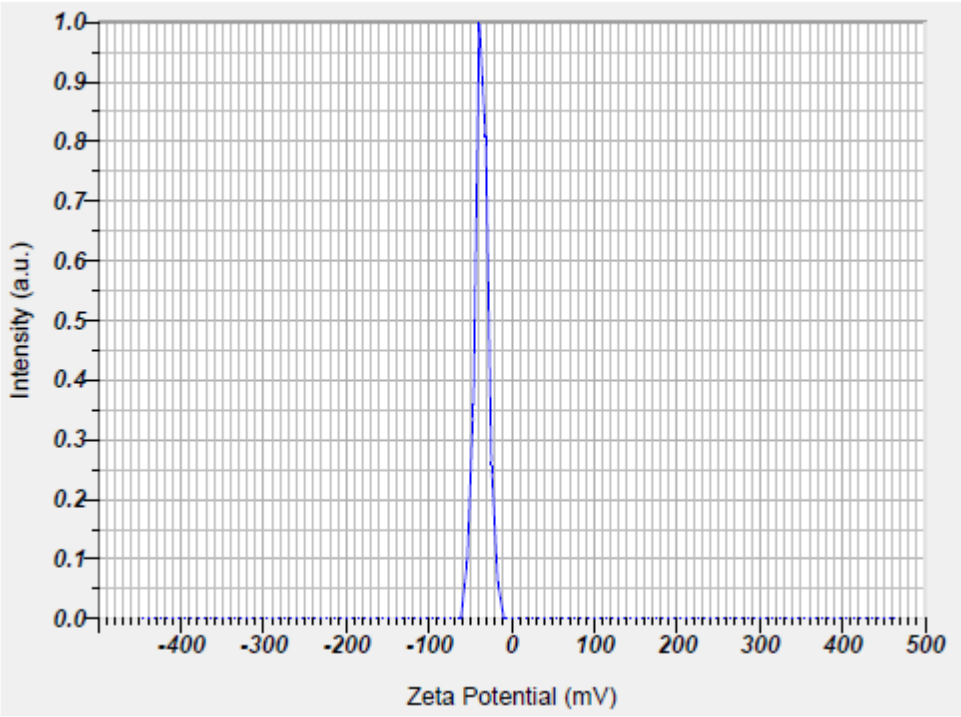

Fig 5 B: Zeta Potential Analysis

This significant negative charge suggests strong electrostatic repulsion between particles, minimizing aggregation and contributing to the stability of the CsSeNP suspension.
Additionally, the electrophoretic mobility was recorded with a mean value of -0.000282 cm²/Vs. This measurement further confirms the stability and effective surface charge of the nanoparticles, as the negative zeta potential aligns with the expectations for chitosan-stabilized selenium nanoparticles, which are suitable for various biomedical and antioxidant applications due to their enhanced dispersion stability.

EDAX Spectrum Analysis

The high carbon and oxygen content primarily corresponds to the chitosan component, confirming its role as the stabilizing matrix for the selenium nanoparticles. The presence of selenium (2.9 wt%) indicates the successful incorporation of selenium into the nanostructure, while the trace amounts of phosphorus, sodium, and zirconium may reflect additional functionalization or residual elements from the synthesis process.
This elemental profile aligns with the intended composition of CsSeNPs, verifying the successful synthesis and elemental integrity of the nanoparticles. The EDX analysis supports the formation of a stable chitosan-selenium nanocomposite, suitable for applications requiring specific elemental compositions for enhanced functionality.

Components	**NAG loaded CSNPs (g/kg diet)**				
	0.0 (Control)	**0.25**	**0.5**	**1.0**	**2.0**
Fish Meal	106	106	106	106	106
Soya bean meal	328	328	328	328	328
Chicken meal	150	150	150	150	150
Groundnut cake	201	201	201	201	201
Wheat bran	104	103.75	103.5	103	102
Codfish oil	21	21	21	21	21
Corn oil	13	13	13	13	13
Vitamins	10	10	10	10	10
Minerals	22	22	22	22	22
Starch	39	39	39	39	39
NAG loaded CSNP's	0.05	0.25	0.5	1.0	2.0
Total	1000	1000	1000	1000	1000
Proximate Chemical analysis (%)					
Dry matter	92.5	91.7	91.8	92.1	91.5
Crude Protein	31.17	32.6	33.15	34.19	33.25
Ether extract	5.2	5.4	5.4	5.3	5.3
Total ash	5.2	5.1	6.4	6.9	6.3
Crude fiber	5.6	5.7	5.8	6.2	6.8
Nitrogen free extract	47.92	47.90	47.95	47.96	47.93
Gross energy (Kcal/100g)	44.5	446.9	453.1	458.4	452.1

Table 1 Chemical composition of feed supplements (% dry weight) containing various levels of N-acetyl-D glucosamine (NAG) loaded chitosan nanoparticles (CSNPs).

Parameters	**NAG loaded CSNPs (g/kg diet)**					**P- value**
	0.0 (Control)	**0.25**	**0.5**	**1.0**	**2.0**	
Initial weight (g)	14.30 ± 0.23	16.63 ± 0.14	14.26 ± 0.08	14.83 ± 0.17	16.73 ± 0.08	<0.046
Final weight (g)	23.33 ± 0.43^{a}	31.73 ± 0.44^{b}	34.80 ± 0.20^{c}	35.3 ± 0.56^{d}	35.17 ± 0.20^{d}	<0.0001
Weight gain (g)	8.033 ± 0.66^{a}	16.37 ± 0.37^{b}	17.25 ± 0.23^{c}	20.47 ± 0.58$^{c, d}$	23.43 ± 0.24^{d}	<0.0001
Weight gain (%)	58.19 ± 5.23^{a}	97.35 ± 3.22^{b}	124.56 ± 1.91^{c}	133.63 ± 4.33$^{c, d}$	133.24 ± 2.07$^{d, e}$	<0.0001
Specific growth rate (SGR) (%)	3.27 ± 0.018 ^{a}	4.38 ± 0.01^{b}	3.53 ± 0.12^{c}	4.57 ± 0.15^{d}	4.28 ± 0.097^{d}	<0.0001
Total food intake (TFI) (g)	29.03 ± 0.94^{a}	31.21 ± 0.98^{b}	38.37 ± 0.68^{c}	41.61 ± 0.55^{d}	39.06 ± 0.43^{d}	<0.0001
Feed conversion ratio (FCR) (g/g)	3.17 ± 0.29^{a}	3.10± 0.11$^{a, b}$	1.73 ± 0.03$^{a, b}$	1.77 ± 0.02$^{a, b}$	2.86 ± 0.03^{b}	<0.145
Protein efficiency ratio (PER) (g/g)	3.14 ± 0.09^{a}	2.32 ± 0.04$^{a, b}$	2.59 ± 0.11^{b}	3.54 ± 0.23^{b}	1.49 ± 0.09^{b}	<0.029
Survival rate (%)	100 ± 0.00	100 ± 0.00	100 ± 0.00	100 ± 0.00	100 ± 0.00	-

Table 2: Growth and feed consumption efficiency of *O. niloticus* supplemented with varying quantitites of N acetyl D glucosamine (NAG) loaded chitosan nanoparticles (CSNPs)

S. No	Microorganisms	Antimicrobial activity		
		CS (mm)	CSNPs (mm)	NAG loaded CSNPs (mm)
1	*Pseudomonas aeruginosa*	11 ± 0.3	14 ± 0.2	22 ± 0.3
2	*Streptococcus agalactiae*	12 ± 0.2	18 ± 0.1	26 ± 0.2
3	*Aeromonas hydrophila*	10 ± 0.3	13 ± 0.3	23 ± 0.4
4	*Pseudomonas fluorescens*	12 ± 0.1	12 ± 0.3	17 ± 0.2
5	Control	NA	NA	NA

Table 3: Antimicrobial assay of chitosan (CS), chitosan nanoparticles (CSNPs), and N-acetyl-D glucosamine (NAG) loaded chitosan nanoparticles (CSNPs) against selected microbial strains.

Discussion

The rapid expansion of aquaculture has highlighted the critical role of feed innovation in sustaining production while minimizing ecological burdens. Traditional reliance on fishmeal and fish oil has been challenged by sustainability concerns, and the use of plant-based proteins, insect meals, and single-cell proteins has emerged as viable alternatives (Hasan et al., 2009; Hardy, 1999). However, these options still face challenges in digestibility, palatability, and nutrient balance, making advanced strategies such as nanotechnology increasingly relevant (Olsen, 2011; Fiorella et al., 2021).Nanoparticle-based interventions have shown considerable promise in enhancing nutrient bioavailability, growth, immunity, and overall aquaculture sustainability (Peters et al., 2016). Among the different classes of nanoparticles, metal-based (zinc, silver, copper), lipid-based (nano-emulsions, SLNs, NLCs), and polymeric forms (chitosan, PLGA) have been successfully incorporated into aquafeeds with beneficial outcomes for fish performance and health (Kumar et al., 2023; Abd El-Hamid et al., 2021; Ghanbary et al., 2022). While these technologies offer distinct advantages, potential concerns regarding environmental accumulation and long-term toxicity remain, necessitating careful evaluation of their safe application (George et al., 2023).

Chitosan nanoparticles (CNPs) stand out for their multifunctional role as immune enhancers, nutrient carriers, and antimicrobial agents. Their biodegradability and muco-adhesive properties allow controlled nutrient release, reducing dependency on antibiotics while improving feed conversion and growth performance (Divya & Jisha, 2018; Kumaran et al., 2020; Akter et al., 2023). Similarly, selenium nanoparticles (SeNPs) have demonstrated superior bioavailability and antioxidant potential compared to conventional selenium supplements, reducing oxidative stress and enhancing disease resistance in fish species (Xiao et al., 2023; Dawood et al., 2021).

Notably, the synergistic formulation of chitosan and selenium nanoparticles represents a significant advancement. This combination improves selenium stability, promotes absorption, and enhances immune responses and muscle quality in Nile tilapia, while simultaneously reducing risks of toxicity (Yazhiniprabha et al., 2022; Abd-Elraoof et al., 2013; Chen et al., 2022). These results indicate that nanoparticle-based supplementation not only improves aquaculture productivity but also offers a sustainable strategy for disease management and environmental protection.Nile tilapia (Oreochromis niloticus) is a model species that provides an excellent platform to evaluate the impact of feed innovations. Its adaptability, rapid growth, and economic importance have led to significant genetic, nutritional, and disease-management research (El-Sayed & Fitzsimmons, 2023; Munguti et al., 2022). The demonstrated benefits of nanoparticle-enhanced feeds in tilapia production highlight their potential scalability across other aquaculture species.

Despite these promising outcomes, several gaps remain. The ecological implications of nanoparticle accumulation in aquatic systems, their interactions with gut microbiota, and potential long-term effects on human consumers require further study. Moreover, the cost-effectiveness of nanoparticle feed additives at commercial scale remains a critical challenge for widespread adoption. Overall, nanoparticle-based feed supplements, particularly chitosan and selenium nanoparticles, offer a forward-looking solution to enhance aquaculture productivity, fish welfare, and sustainability. Their integration into commercial feeds must be accompanied by rigorous safety assessments, life-cycle analyses, and cost-benefit evaluations to ensure long-term viability. Future research should prioritize optimizing formulations, scaling up production methods, and investigating the combined effects of nanoparticles with other emerging feed ingredients, such as insect meals and algae-based proteins.

References

1. Abd El-Hamid MI, Ibrahim SM, Eldemery F, El-Mandrawy SA, Metwally AS, Khalifa E, Elnahriry SS, Ibrahim D. Dietary cinnamaldehyde nanoemulsion boosts growth and transcriptomes of antioxidant and immune related genes to fight *Streptococcus agalactiae* infection in *Nile tilapia* (*Oreochromis niloticus*). Fish & Shellfish Immunology. 2021 Jun 1;113:96-105.
2. Abd El-Naby AS, Al-Sagheer AA, Negm SS, Naiel MA. Dietary combination of chitosan nanoparticle and thymol affects feed utilization, digestive enzymes, antioxidant status, and intestinal morphology of *Oreochromis niloticus*. Aquaculture. 2020 Jan 15;515:734577.

3. Abdel-Ghany HM, Salem ME. Effects of dietary chitosan supplementation on farmed fish; a review. Reviews in Aquaculture. 2020 Feb;12(1):438-52.
4. Abd-Elraoof WA, Tayel AA, Shaymaa W, Abukhatwah OM, Diab AM, Abonama OM, Assas MA, Abdella A. Characterization and antimicrobial activity of a chitosan-selenium nanocomposite biosynthesized using Posidonia oceanica. RSC advances. 2023;13(37):26001-14.
5. Adel Abdel-Khalek A, Kadry M, Hamed A, Marie MA. Ecotoxicological impacts of zinc metal in comparison to its nanoparticles in *Nile tilapia*; *Oreochromis niloticus*. The Journal of Basic & Applied Zoology. 2015 Oct 1;72:113-25.
6. Akter N, Jewel MA, Haque MA, Nahiduzzaman M, Rahman MH, Khatun MB, Satter A. Effects of dietary Cu nanoparticles on growth performance, physiology and bioaccumulation in Asian walking catfish (*Clarias batrachus*). Archives of Agriculture and Environmental Science. 2023 Sep 25;8(3):427-36
7. Anderson JL, Asche F, Garlock T, Chu J. Aquaculture: Its role in the future of food. In World agricultural resources and food security: International food security 2017 Jul 15 (pp. 159-173). Emerald Publishing Limited.
8. Bano I, Skalickova S, Sajjad H, Skladanka J, Horky P. Uses of selenium nanoparticles in the plant production. Agronomy. 2021 Nov 3;11(11):2229.
9. Bashar A, Hasan NA, Haque MM, Rohani MF, Hossain MS. Effects of dietary silica nanoparticle on growth performance, protein digestibility, hematology, digestive morphology, and muscle composition of *Nile tilapia*, *Oreochromis niloticus*. Frontiers in Marine Science. 2021 Aug 17;8:706179.
10. Bashir SM, Ahmed Rather G, Patrício A, Haq Z, Sheikh AA, Shah MZ, Singh H, Khan AA, Imtiyaz S, Ahmad SB, Nabi S. Chitosan nanoparticles: a versatile platform for biomedical applications. Materials. 2022 Sep 20;15(19):6521.
11. Bisht N, Phalswal P, Khanna PK. Selenium nanoparticles: A review on synthesis and biomedical applications. Materials Advances. 2022;3(3):1415-31.
12. Bostock J, McAndrew B, Richards R, Jauncey K, Telfer T, Lorenzen K, Little D, Ross L, Handisyde N, Gatward I, Corner R. Aquaculture: global status and trends. Philosophical Transactions of the Royal Society B: Biological Sciences. 2010 Sep 27;365(1554):2897-912.
13. Chen W, Li X, Cheng H, Xia W. Chitosan-based selenium composites as potent Se supplements: Synthesis, beneficial health effects, and applications in food and agriculture. Trends in Food Science & Technology. 2022 Nov 1;129:339-52.
14. Chouhan D, Mandal P. Applications of chitosan and chitosan based metallic nanoparticles in agrosciences-A review. International journal of biological macromolecules. 2021 Jan 1;166:1554-69.
15. Dawood MA, Basuini MF, Yilmaz S, Abdel-Latif HM, Kari ZA, Abdul Razab MK, Ahmed HA, Alagawany M, Gewaily MS. Selenium nanoparticles as a natural antioxidant and metabolic regulator in aquaculture: a review. Antioxidants. 2021 Aug 27;10(9):1364.
16. Dawood MA, Eweedah NM, Moustafa EM, El-Sharawy ME, Soliman AA, Amer AA, Atia MH. Copper nanoparticles mitigate the growth, immunity, and oxidation resistance in common carp (*Cyprinus carpio*). Biological trace element research. 2020 Nov;198:283-92.
17. Dawood MA, Zommara M, Eweedah NM, Helal AI. Synergistic effects of selenium nanoparticles and vitamin E on growth, immune-related gene expression, and regulation of antioxidant status of *Nile tilapia* (*Oreochromis niloticus*). Biological trace element research. 2020 Jun;195:624-35.
18. De Silva C, Nawawi NM, Abd Karim MM, Abd Gani S, Masarudin MJ, Gunasekaran B, Ahmad SA. The mechanistic action of biosynthesized silver nanoparticles and its application in aquaculture and livestock industries. Animals. 2021 Jul 14;11(7):2097.
19. Divya K, Jisha MS. Chitosan nanoparticles preparation and applications. Environmental chemistry letters. 2018 Mar;16:101-12.
20. El-Sayed AF, Fitzsimmons K. From Africa to the world—The journey of *Nile tilapia*. Reviews in Aquaculture. 2023 Feb;15:6-21.
21. El-Sayed AF. Effects of stocking density and feeding levels on growth and feed efficiency of *Nile tilapia* (*Oreochromis niloticus* L.) fry. Aquaculture research. 2002 Jul;33(8):621-6.
22. Fiorella KJ, Okronipa H, Baker K, Heilpern S. Contemporary aquaculture: implications for human nutrition. Current Opinion in Biotechnology. 2021 Aug 1;70:83-90.
23. Garg U, Chauhan S, Nagaich U, Jain N. Current advances in chitosan nanoparticles based drug delivery and targeting. Advanced pharmaceutical bulletin. 2019 Jun;9(2):195.
24. George D, Lakshmi S, Sharma A, Prakash S, Siddiqui M, Malavika BR, Elumalai P. Nanotechnology: A novel tool for aquaculture feed development. InNanotechnological Approaches to the Advancement of Innovations in Aquaculture 2023 Mar 28 (pp. 67-88). Cham: Springer International Publishing.
25. Ghanbary K, Firouzbakhsh F, Arkan E, Mojarrab M. The effect of *Thymbra spicata* hydroalcoholic extract loaded on chitosan polymeric nanoparticles on some growth performances, hematology, immunity, and response to acute stress in rainbow trout (*Oncorhynchus mykiss*). Aquaculture. 2022 Feb 15;548:737568.

26. Gonzales Jr JM, Brown PB. *Nile tilapiaOreochromis niloticus* as a food source in advanced life support systems: Initial considerations. Advances in Space Research. 2006 Jan 1;38(6):1132-7.
27. Hardy RW. Collaborative opportunities between fish nutrition and other disciplines in aquaculture: an overview. Aquaculture. 1999 Jul 1;177(1-4):217-30.
28. Hasan MR, Halwart M. Fish and feed inputs for aquaculture. Practices, sustainability and implications., FAO Fisheries and aquaculture technical paper. 2009;518.
29. Hoerterer C, Petereit J, Lannig G, Johansen J, Pereira GV, Conceição LE, Pastres R, Buck BH. Sustainable fish feeds: the potential of emerging protein sources in diets for juvenile turbot (*Scophthalmus maximus*) in RAS. Aquaculture International. 2022 Jun;30(3):1481-504.
30. Holmes AB, Gu FX. Emerging nanomaterials for the application of selenium removal for wastewater treatment. Environmental Science: Nano. 2016;3(5):982-96.
31. Joshi HD, Tiwari VK, Gupta S, Sharma R, Lakra WS, Sahoo U. Application of nanotechnology for the production of masculinized Tilapia, *Oreochromis niloticus* (Linnaeus, 1758). Aquaculture. 2019 Sep 15;511:734206.
32. Korni FM, Mohammed AN, Moawad UK. Using some natural essential oils and their nano-emulsions for ammonia management, anti-stress and prevention of streptococcosis in *Nile tilapia*, *Oreochromis niloticus*. Aquaculture International. 2023 Aug;31(4):2179-98.
33. Krishnaraj C, Radhakrishnan S, Ramachandran R, Ramesh T, Kim BS, Yun SI. In vitro toxicological assessment and biosensing potential of bioinspired chitosan nanoparticles, selenium nanoparticles, chitosan/selenium nanocomposites, silver nanoparticles and chitosan/silver nanocomposites. Chemosphere. 2022 Aug 1;301:134790.
34. Kumar N, Thorat ST, Patole PB, Gite A, Kumar T. Does selenium and zinc nanoparticles support mitigation of multiple-stress in aquaculture? Aquaculture. 2023 Jan 30;563:739004.
35. Kumaran S, Aruni W, Karthik M. Trends in aquaculture feed development with chitosan nano particles–a review. BiosciBiotechnol Res Commun. 2020;13(10.21786).
36. Leonard JN, Skov PV. Capacity for thermal adaptation in *Nile tilapia* (*Oreochromis niloticus*): Effects on oxygen uptake and ventilation. Journal of Thermal Biology. 2022 Apr 1;105:103206.
37. Mair GC, Halwart M, Derun Y, Costa-Pierce BA. A decadal outlook for global aquaculture. Journal of the World Aquaculture Society. 2023 Apr 1;54(2).
38. Munguti JM, Nairuti R, Iteba JO, Obiero KO, Kyule D, Opiyo MA, Abwao J, Kirimi JG, Outa N, Muthoka M, Githukia CM. *Nile tilapia* (*Oreochromis niloticus* Linnaeus, 1758) culture in Kenya: Emerging production technologies and socio-economic impacts on local livelihoods. Aquaculture, Fish and Fisheries. 2022 Aug;2(4):265-76.
39. Mustafa S, Estim A, Shapawi R, Shalehand MJ, Sidik SR. Technological applications and adaptations in aquaculture for progress towards sustainable development and seafood security. InIOP Conference Series: Earth and Environmental Science 2021 Mar 1 (Vol. 718, No. 1, p. 012041). IOP Publishing.
40. Naylor RL, Hardy RW, Bureau DP, Chiu A, Elliott M, Farrell AP, Forster I, Gatlin DM, Goldburg RJ, Hua K, Nichols PD. Feeding aquaculture in an era of finite resources. Proceedings of the National Academy of Sciences. 2009 Sep 8;106(36):15103-10.
41. Nyakeya K, Chemoiwa E, Nyamora JM, Ogombe CO, Gichana ZM, Mbaru EK, Masese FO, Aura CM, Nyamweya C, Njiru J, Ondiba R. Endemic Lake Baringo *Oreochromis niloticus* fishery on verge of collapse: Review of causes and strategies directed to its recovery, conservation and management for sustainable exploitation. Lakes & Reservoirs: Research & Management. 2020 Dec;25(4):423-38.
42. Olivera S, Muralidhara HB, Venkatesh K, Guna VK, Gopalakrishna K, Kumar Y. Potential applications of cellulose and chitosan nanoparticles/composites in wastewater treatment: a review. Carbohydrate polymers. 2016 Nov 20;153:600-18.
43. Olsen Y. Resources for fish feed in future mariculture. Aquaculture Environment Interactions. 2011 Mar 10;1(3):187-200
44. Partridge GJ, Rao S, Woolley LD, Pilmer L, Lymbery AJ, Prestidge CA. Bioavailability and palatability of praziquantel incorporated into solid-lipid nanoparticles fed to yellowtail kingfish *Seriola lalandi*. Comparative Biochemistry and Physiology Part C: Toxicology & Pharmacology. 2019 Apr 1;218:14-20.
45. Peters RJ, Bouwmeester H, Gottardo S, Amenta V, Arena M, Brandhoff P, Marvin HJ, Mech A, Moniz FB, Pesudo LQ, Rauscher H. Nanomaterials for products and application in agriculture, feed and food. Trends in Food Science & Technology. 2016 Aug 1;54:155-64.
46. Phan LT, Bui TM, Nguyen TT, Gooley GJ, Ingram BA, Nguyen HV, Nguyen PT, De Silva SS. Current status of farming practices of striped catfish, Pangasianodon hypothalamus in the Mekong Delta, Vietnam. Aquaculture. 2009 Nov 16;296(3-4):227-36.
47. Samrongpan, C., N. Areechon, R. Yoonpundh, and P. Srisapoome. "Effects of mannan-oligosaccharide on growth, survival and disease resistance of Nile tilapia (Oreochromis niloticus Linnaeus) fry." (2008): 345-353.Prabu E, Rajagopalsamy CB, Ahilan B, Jeevagan IJ, Renuhadevi MJ. *Tilapia*–an excellent candidate species for world aquaculture: a review. Annual Research & Review in Biology. 2019 Mar 29;31(3):1-4.

48. Sarkar B, Bhattacharjee S, Daware A, Tribedi P, Krishnani KK, Minhas PS. Selenium nanoparticles for stress-resilient fish and livestock. Nanoscale research letters. 2015 Dec;10:1-4.
49. Sharjeel M, Ali S, Summer M, Noor S, Nazakat L. Recent advancements of nanotechnology in fish aquaculture: an updated mechanistic insight from disease management, growth to toxicity. Aquaculture International. 2024 Apr 1:1-38.
50. Terzioğlu P, Öğüt H, Kalemtaş A. Natural calcium phosphates from fish bones and their potential biomedical applications. Materials Science and Engineering: C. 2018 Oct 1;91:899-911.
51. Tesfahun A, Temesgen M. Food and feeding habits of *Nile tilapiaOreochromisniloticus(L.)* in Ethiopian water bodies: A review. International Journal of Fisheries and Aquatic Studies. 2018;6(1):43-7.
52. Thangapandiyan S, Monika S. Green synthesized zinc oxide nanoparticles as feed additives to improve growth, biochemical, and hematological parameters in freshwater fish *Labeorohita*. Biological trace element research. 2020 Jun;195:636-47.
53. Vijayakumar S, Chen J, Divya M, Durán-Lara EF, Prasannakumar M, Vaseeharan B. A review on biogenic synthesis of selenium nanoparticles and its biological applications. Journal of Inorganic and Organometallic Polymers and Materials. 2022 Jul;32(7):2355-70.
54. Wang SY, Herrera-Balandrano DD, Jiang YH, Shi XC, Chen X, Liu FQ, Laborda P. Application of chitosan nanoparticles in quality and preservation of postharvest fruits and vegetables: A review. Comprehensive Reviews in Food Science and Food Safety. 2023 May;22(3):1722-62.
55. Xiao X, Deng H, Lin X, Ali ASM, Viscardi A, Guo Z, Qiao L, He Y, Han J. Selenium nanoparticles: Properties, preparation methods, and therapeutic applications. Chem Biol Interact. 2023 Jun 1;378:110483. doi: 10.1016/j.cbi.2023.110483
56. Yazhiniprabha M, Gopi N, Mahboob S, Al-Ghanim KA, Al-Misned F, Ahmed Z, Riaz MN, Sivakamavalli J, Govindarajan M, Vaseeharan B. The dietary supplementation of zinc oxide and selenium nanoparticles enhance the immune response in freshwater fish *Oreochromis mossambicus* against aquatic pathogen *Aeromonas hydrophila*. Journal of Trace Elements in Medicine and Biology. 2022 Jan 1;69:126878.
57. Zhou C, Xu D, Lin K, Sun C, Yang X. Intelligent feeding control methods in aquaculture with an emphasis on fish: a review. Reviews in Aquaculture. 2018 Dec;10(4):975-93.
.